International Workshop on

The Application of Nanocrystalline Diamond Like Carbon Materials

IWAncDLC-2006

Nov 28 - Dec 01, 2006

Edited by

Nihar Ranjan Ray

Co-editors

Md. Nurujjaman
Ramesh Narayanan
Abhijit Betal
Ramitendranath Bhattacharyya

Organized by

Saha Institute of Nuclear Physics
Kolkata, India

Biomedical Behavior and Biocompatibility of Diamond-like-Carbon (DLC) Films

***Ricky K. Y. Fu*, S. C. H. Kwok and Paul K. Chu**

Abstract : Diamond-like-carbon (DLC) is an attractive biomedical material due to its high inertness and excellent mechanical properties. It is being used in many biomedical applications such as blood contacting-devices including rotary blood pumps, mechanical heart valves, coronary artery stents, and heart valve replacements. Using plasma-based technology such as plasma implantation and deposition, various types of DLC and doped DLC films under different conditions have been produced. The properties of the films are affected by the implantation and deposition parameters such as precursors flow rate, bias voltage, temperature and dopant element and concentration. The film characteristics and structures have been investigated and have been correlated to the *in vitro* hemocompatibilty and biomedical behaviors. The composition, sp^3/sp^2 ratio, surface morphology, surface energy, electrical and semiconductor properties of the DLC and doped DLC films have been studied and used to interpret the biocompatible mechanism such as the adhesion, activation, and morphology of the platelets as well as anticoagulation properties.

Keywords : Diamond-like Carbon; Blood Compatibility; Ion Implantation and Deposition

1. Introduction

DLC thin films have been widely studied and used in many industrial purposes in the past twenty years due to their superior chemical, optical, electrical, and tribological properties. Their particularly favorable attributes include low friction coefficient, high hardness and wear resistance. They have been used commercially as the coating materials in many applications, for instance shavers, cutting and drilling tools, protective coating for magnetic media and optical lenses. However, there has also been a lot of interest in DLC as biomedical coating materials since the materials not only possess excellent chemical and mechanical properties, but also are in general biocompatible [1-3]. Conventionally, metals or metal alloys are the dominant materials in medical implants. But relatively poor wear and corrosion resistance and inadequate biocompatibility are the drawbacks of some metallic materials. Therefore, DLC has been suggested to be a replacement in some applications. However, entire substitution of most medical devices with DLC is not practical. Thus, surface modification approach such as coating techniques is one of the potential solutions.

Initial studies of DLC in biomedical applications were mainly applied for the orthopedic field such as surface modification of artificial total hip and knee joints [4-7]. Most studies show that the DLC films are biocompatibility, and most important that the tribological properties can be greatly improved by coating with the DLC films. However, for the cardiovascular field, there are fewer literature reports. Referring to the commercial products of cardiovascular devices such as artificial heart valves, rotary heart pumps, and stents, the crucial requirement of biocompatibility is the bioinertness to blood. In other words, the implants must avoid the occurrence of thrombogenesis. In practice, the haemocompatibility of the devices is not adequate, the

[a] Department of Physics & Materials Science, City University of Hong Kong, Tat Chee Avenue, Kowloon, Hong Kong,

patients should continuously take anticoagulation medication after receiving implants. Hence the development of a material with better blood compatibility is necessary.

In this study, elemental doped and un-doped DLC films are prepared by plasma immersion ion implantation and deposition technique under different processing parameters. The film properties related to the blood compatibility are characterized and compared.

2. Biomedical test procedures for DLC

To estimate the haemocompatibility of the DLC films, the *in-vitro* platelet adhesive test was applied. It is one of the direct and efficient approaches to evaluate the blood compatibility of the materials. The technique assesses the surface thrombogenicity of the element doped DLC films and examines the interaction between the materials and blood. Fig. 1 describes the procedures of the test. Initially, the fresh blood plasma was collected from a healthy adult and sent to the laboratory within 24 hours. The yellow fluid platelet rich plasma (PRP) was then obtained after the blood had been centrifuged for 15 minutes at 1000 revolution per minute. On the other hand, the prepared samples in about 5×5 mm^2 (cleaned with the ultrasonic bath) were placed in a flat container and the PRP solution was flowed into the container. The samples were immersed in the PRP solution and incubated at 37°C (simulated to human body temperature) for 15 and 120 minutes separately. The platelets contacted with the DLC films, interacted and eventually adhered on the surface of the films. After rinsing, fixing, and critical point drying, the specimens were examined using optical microscopy (OM) and scanning electron microscopy (SEM). By employing the point counting method at a fixed magnification factor, the quantity and morphology of the adherent platelets were determined to assess platelet adhesion and activation respectively. Ten fields on each sample were chosen randomly to obtain the statistical averages of the total number of adherent and activated platelets.

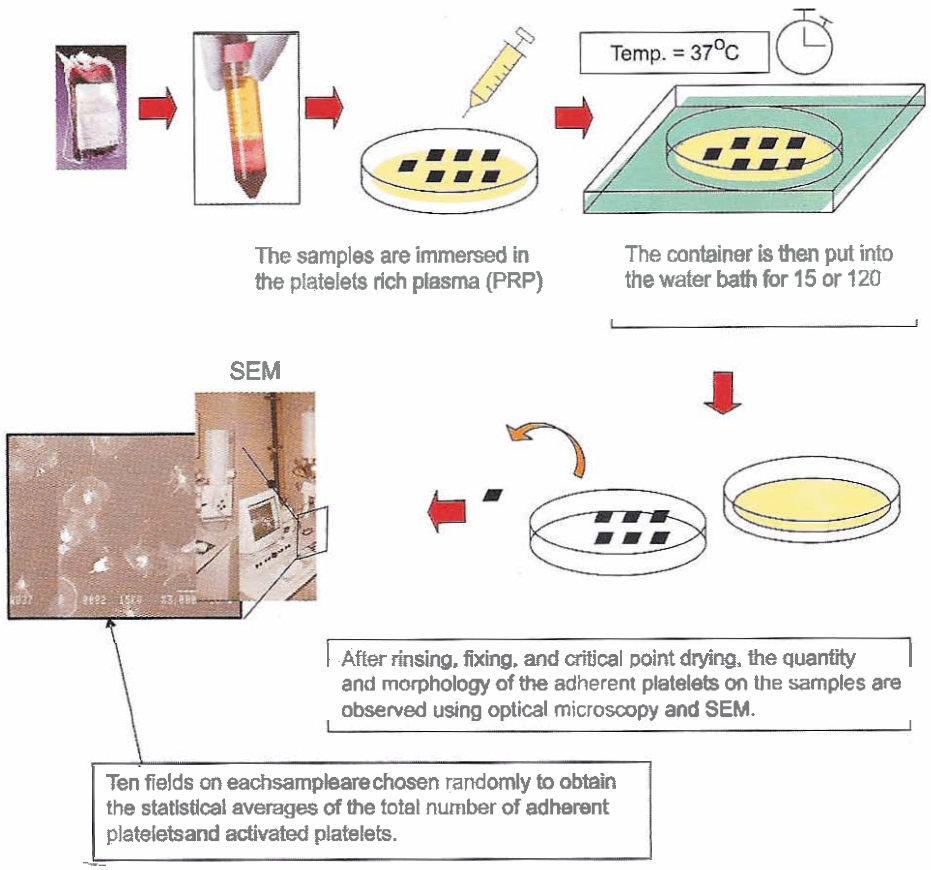

Fig. 1. Schematic diagram of the experimental procedure of platelet adhesion test.

3. Analysis of platelets adhesion test

To identify the adherent and activated platelets, one can observe the morphology of the adherent platelets. Fig. 2 shows SEM micrograph of typical activated and non-activated platelets on the same surface.

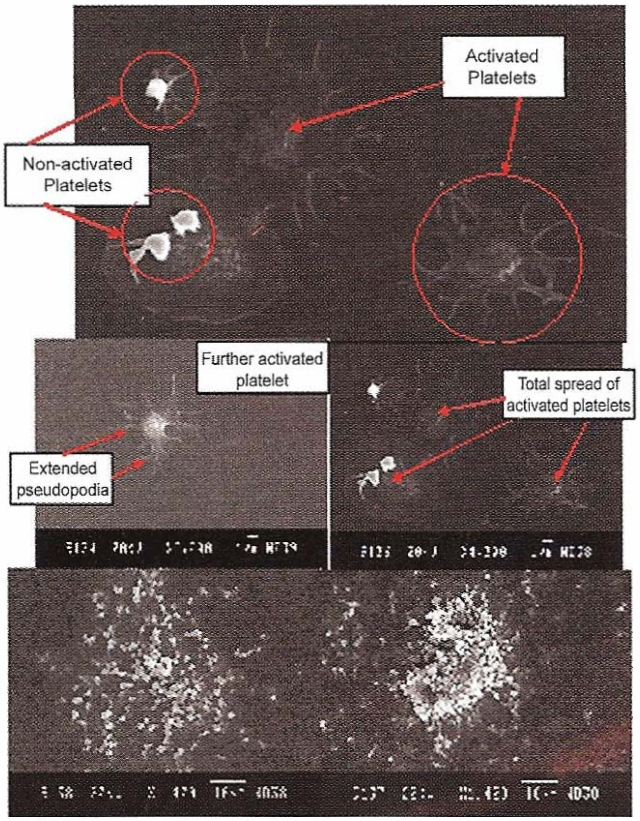

Fig. 2. SEM micrograph of typical activated and non-activated adherent platelets on the same surface.

The non-activated platelets typically manifest as disk-shaped cells about 2-3 μm in size. Slight pseudopodia indicate the early stage of activation. A different morphology exhibiting heavily developed pseudopodia, large size (>5 μm), and more depressed shape indicates a high state of activation of adherent platelet. In the serious case platelets aggregate after activated on the substrate surface.

4. DLC fabrication techniques

The samples of un-doped and doped DLC films were fabricated by utilizing the plasma immersion ion implantation and deposition (PIII-D). For PIII-D method, the acetylene (C_2H_2) gas was applied to produce the carbon plasma for film deposition. While the dopants were introduced into the vacuum chamber simultaneously via thermal or electron the impact evaporation approach. Phosphorus and calcium doped DLC films were fabricated by using this method. C_2H_2 and Ar gases are bled into the chamber through two individual flow controls and inlets on top of the chamber. Fig. 3 illustrates the schematic diagram of the basic experimental setup

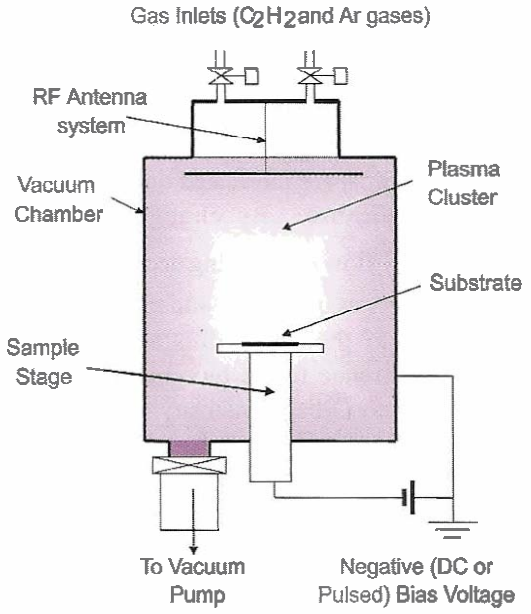

Fig. 3. Schematic diagram of PIII-D system for DLC synthesis.

of PIII-D for DLC films synthesis. By using the PIII-D system with C_2H_2, amorphous hydrogenated carbon films can be produced. For elemental doped DLC films fabrication, however, additional dopant source is equipped with the system to provide additional ions for

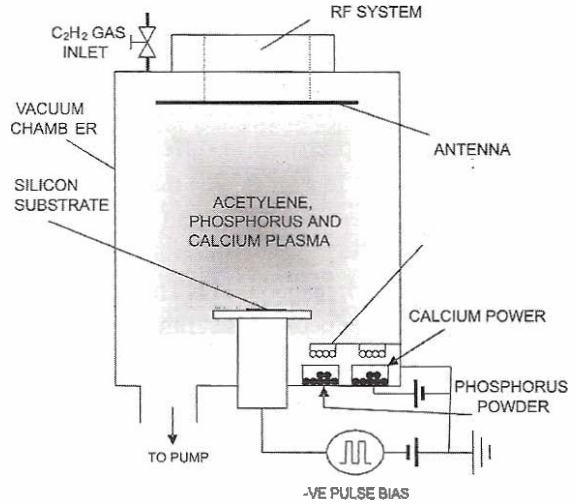

Fig. 4. Schematic diagram of PIII-D to deposit Ca, Ca & P, and P doped DLC films.

film deposition. In general cases, the powder of the element is placed in a container and evaporated by means of heated filament and electron bombardment. The dopant vapor is created, mixed with the C_2H_2 gas, and eventually ignited into plasma by RF sources for film deposition as demonstrated in Fig. 4.

5. Blood platelet behaviors on DLC

5.1 The influence of flow rate on film characteristics

Using plasma immersion ion implantation - deposition (PIII-D), DLC films are fabricated on silicon substrates at room temperature. By changing the C_2H_2 to $Ar\left(F_{C_2H_2}/F_{Ar}\right)$ flow ratio during deposition, the effects of the reactive gas pressure and flow ratio on the characteristics of the DLC films are systematically examined to correlate to the blood compatibility. The Raman D-band to G-band intensity ratio is consistent with the adherent platelet quantity. Both first increase and then decrease with higher $F_{C_2H_2}/F_{Ar}$ flow ratios. This implies that the blood compatibility of the DLC films is influenced by the ratio of sp^3 to sp^2, not by the absolute sp^3 or sp^2 content.

Using stylus profilometry, the film thicknesses are determined to be about 100, 130, 200, 240, and 300 nm at $F_{C_2H_2}/F_{Ar}$ flow ratios of 0.4, 0.6, 0.8, 1.0, and 1.2, respectively. As expected, the deposition rate is higher with increasing C_2H_2 flow rate. Fig. 5 exhibits the three-dimensional AFM morphology of the DLC films at $F_{C_2H_2}/F_{Ar}$ flow ratios of 0.6 and 1.2. The surfaces are relatively smooth, but a higher $F_{C_2H_2}/F_{Ar}$ flow ratio gives rise to a rougher surface, and it is due to the difference in the sp3 content. The Raman spectra acquired from the DLC films prepared at different $F_{C_2H_2}/F_{Ar}$ flow ratios are shown in Fig. 6. All the Raman spectra show a relatively sharp peak at around 1550 cm^{-1} and a shoulder at around 1345 cm^{-1}, commonly referred to as the G band and D band, respectively. The latter becomes a shoulder of the former because the film is hydrogenated. It is found that the shifts of both the G and D peaks are the biggest and the G-peak width [full width half maximum (FWHM)] is the largest at a $F_{C_2H_2}/F_{Ar}$ flow ratio of 1.2. The changes in the Raman spectra indicate that smaller $F_{C_2H_2}/F_{Ar}$ flow ratios weaken the formation of DLC films with more fourfold coordinate bonds. That is, the sp^3 bond content is reduced at smaller $F_{C_2H_2}/F_{Ar}$ flow ratios. The peak width and I_D/I_G intensity ratio both vary depending on the structure of the DLC films.

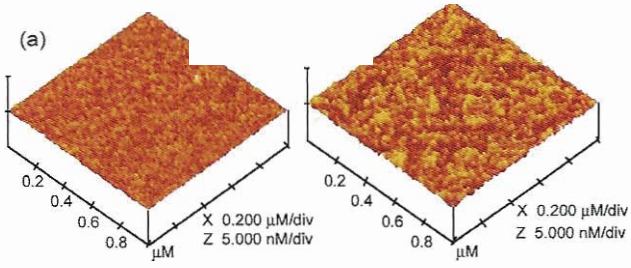

Fig. 5. AFM micrographs of the DLC films prepared by PIII-D at $F_{C_2H_2}/F_{Ar}$ ratios of (a) 0.6 and (b) 1.2.

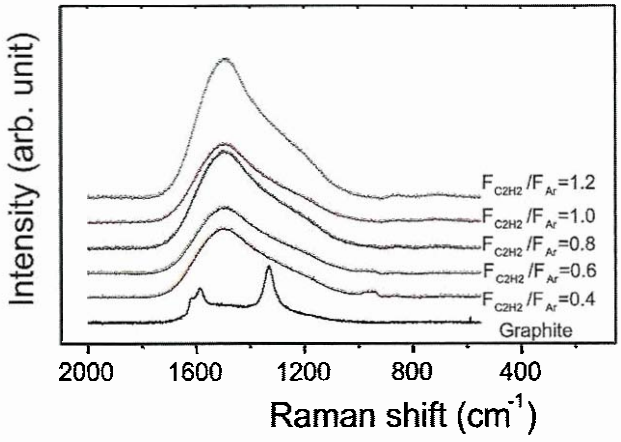

Fig. 6. Raman spectra of DLC films fabricated at different $F_{C_2H_2}/F_{Ar}$ ratios.

The platelet adhesion tests are conducted on the DLC film surface. After incubation in PRP for 20 minutes, the number of adherent platelets on the DLC film surface first increases, and then decreases with increasing of $F_{C_2H_2}/F_{Ar}$ flow ratios. The platelet count is highest at a $F_{C_2H_2}/F_{Ar}$ flow ratio of about 0.8. After 3 hours of incubation, the adherent platelets are too numerous to count.

The amount of platelets on sample prepared under $F_{C_2H_2}/F_{Ar}$ flow ratio of 0.8 is the highest, and the accumulation of platelets is also most serious as manifested by several platelets interconnecting to form aggregation. In addition, pseudopodium of the adhered platelets is also observed seriously on this sample.

Fig. 7 displays the relationship between the Raman D-band to G-band intensity ratios and the platelet quantity for different $F_{C_2H_2}/F_{Ar}$ flow ratios. It can be readily observed that these two parameters agree well with each other. That is, both increase first and then decrease with increasing $F_{C_2H_2}/F_{Ar}$ flow ratios. The largest value is observed at a $F_{C_2H_2}/F_{Ar}$ flow ratio of 0.8 - 1.0. Taking into the account the Raman results shown in Fig. 6 which illustrates that the shift of both the G and D peaks is the biggest and the FWHM of the G-band peak is largest at a $F_{C_2H_2}/F_{Ar}$ flow ratio of 1.2, it can be inferred that the blood compatibility of the DLC film is influenced by the sp^3 to sp^2 ratio, not by the absolute sp^3 content or sp^2 content, and the hemo-compatibility becomes worse when the sp^3 to sp^2 ratio increases.

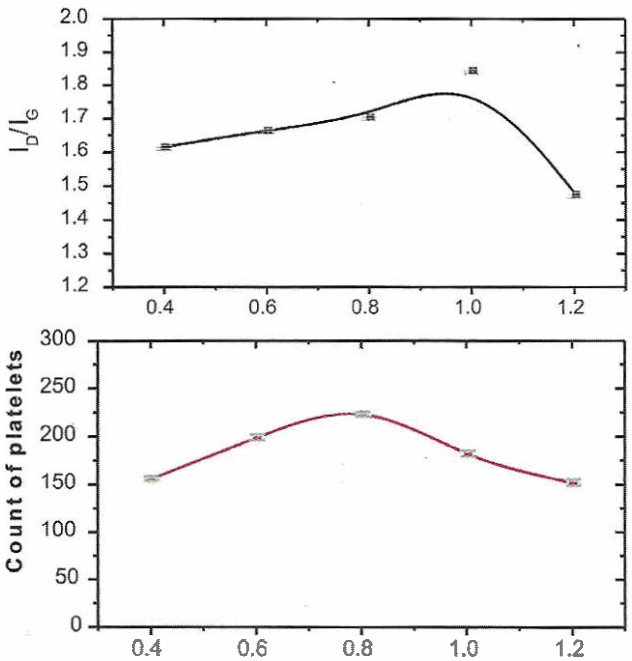

Fig. 7. Effects of the $F_{C_2H_2}/F_{Ar}$ flow ratios on the intensity ratio of the D-band to G-band and platelet counts

5.2 The influence of bias voltage on film characteristics

Hydrogenated amorphous carbon films were fabricated at room temperature. A mixture of acetylene (C_2H_2) and argon was subsequently introduced into the chamber and the plasma was triggered using radio frequency (RF). Film deposition was carried out at a constant RF power of 500 W. During the initial deposition of the base film, a higher negative DC bias voltage was applied to the sample holder to improve film adhesion by means of ion mixing. A series of DLC films were synthesized by adjusting the substrate bias voltage in subsequent deposition of the top films.

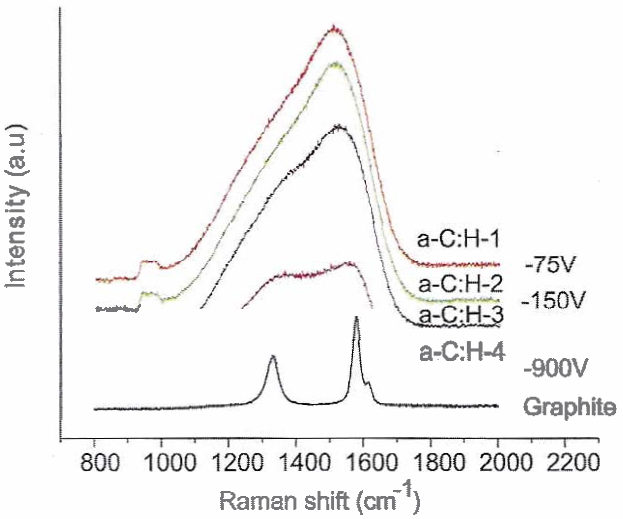

Fig. 8. Raman spectra of the a-C:H films fabricated at different bias voltages.

The Raman spectra acquired from the hydrogenated DLC (a-C:H) films prepared under different bias voltages are exhibited in Fig. 8. A higher bias voltage (V_b) leads to shifts of the two peaks towards higher wave numbers and increasing I_D/I_G ratios. The positions of the G and D-lines, G-full width at half-maximum and integrated intensity ratio (I_D/I_G) can be correlated with the sp^3/sp^2 bonding ratio [8], graphite cluster size [9,10], and disorder in these threefold coordinated islands [11]. Hence, the sp^3/sp^2 ratios in the a-C:H films cannot be derived directly from the Raman spectra, but nevertheless, some qualitative information can be extracted. Increases in the I_D/I_G ratio, shifting of the G-peak towards higher wave numbers, widening of the D-peak, and narrowing of the G-peak are caused by increase of the graphite-like component in the amorphous carbon films [12]. The results indicate that the film structure becomes more graphite like with increasing substrate bias. One of the reasons is that the increase in substrate temperature induced by higher energetic ion bombardment promotes film graphitization, as it has been shown that such a graphitization process is thermally driven [13].

Wettability examinations were performed using the sessile drop method.

$$\left(\gamma_1^p\gamma_s^p\right)^{1/2}+\left(\gamma_1^d\gamma_s^d\right)^{1/2}=\gamma_1(1+\cos\theta)$$

where γ_s^p and γ_s^p are the polar and dispersive components of the solid phases. The polar and dispersive components of the investigated coatings were determined by a contact angle measurement using six different liquids.

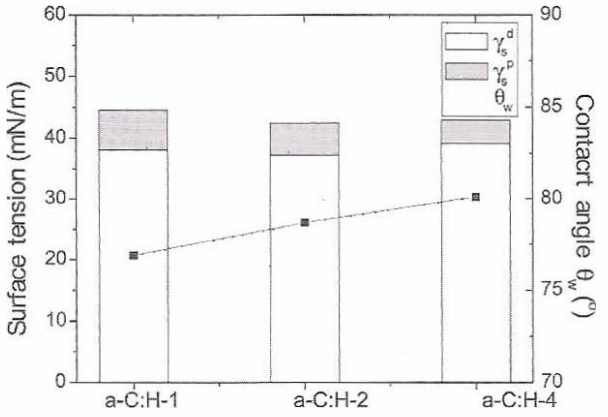

Fig. 9. Surface energies (γ_s) and their polar and dispersive components (γ_s^p and γ_s^d) of the a-C:H films.

The surface energy (γ_s) and its polar and dispersive components (γ_s^p and γ_s^d) are shown in Fig. 9 together with the contact angle of water. The results show that all the surfaces have a hydrophobic nature with much higher γ_s^d than γ_s^p. As the absolute value of the bias voltage increases, the polar part of the surface energy decreases by nearly 60% from 6.4 mJ/m^2 to 3.8 mJ/m^2. The contact angle of water for the films is about 75° – 85° and decreases with higher V_b. The trends are consistent with the change of the I_D/I_G ratio as displayed in Fig. 10. The

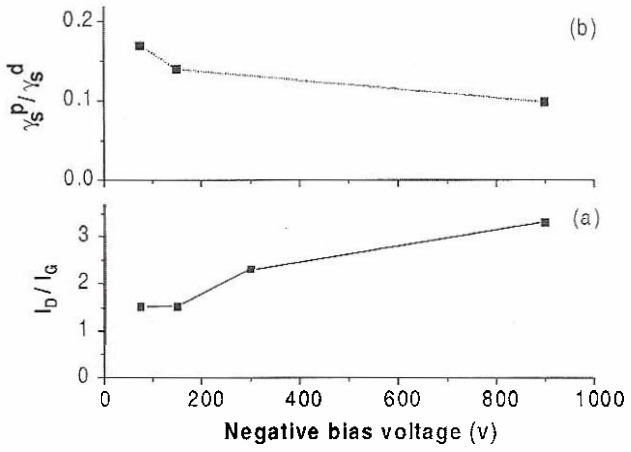

Fig. 10. Effects of the bias voltage on: (a) Intensity ratio of the D-band to G-band and (b) Ratio of polar/ dispersive component of the surface energy.

surface energy thus appears to be affected mainly by the sp^3 content in the films, and Pinzari's study on the wettability of diamond films in fact showed similar effects [14].

Fig. 11 exhibits the statistical results of the platelets adhered on the a-C:H film surfaces from PRP, expressed as a percentage of platelets adhered on the stainless steel in the same test. After incubation in PRP for 15 minutes, the number of adherent platelets slightly decreases with increasing V_b (absolute value) and is less than that on stainless steel surface. The percentage of un-activated platelets drops steeply from 30% to 8% when V_b is changed from –75 V to –900 V. The percentage of un-activated platelets on stainless steel is in between.

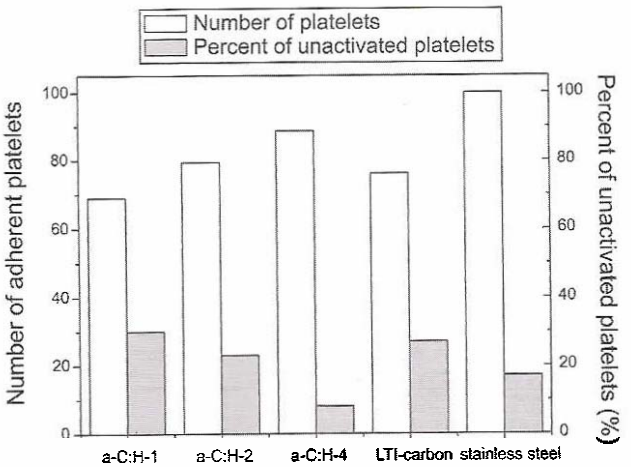

Fig. 11. Quantity of platelets adhered on the surface of the a-C:H films synthesized at different bias voltages (15 minutes incubation in PRP) [Expressed as a percentage of platelets adhering on the stainless steel in the same test].

Platelets are strongly surface activated by the a-C:H film deposited at high V_b (absolute value) compared to those at low V_b (absolute value). It is consistent with the variation of the polar component γ_s^p of the surface energy. The platelet attachment studies suggest that the adhesion behavior of the platelets is related to the surface energy of the film. The higher the absolute value of V_b, the lower is the value of γ_s^p, and accordingly, the higher the activation of adherent platelets. Besides, the results show that when the bias V_b (absolute value) is increased, the interfacial energy of albumin and fibrinogen increases from 10.8 mJ/m^2 and 15.0 mJ/m^2 to 15.9 mJ/m^2 and 20.9 mJ/m^2, respectively. It is expected because protein molecules will undergo a conformational transformation when plasma protein adsorbs onto an artificial surface

(higher interfacial energy) from its aqueous phase (lower interfacial energy). Thus, it suggests that the higher the interfacial energy γ_{sp}, the larger the conformation changes. Moreover, the exacerbation of activation of the platelets adhered on the a-C:H film deposited at high V_b is probably due to the changes of fibrinogen conformation.

All in all, the study of *the surface energy of the films* shows that the polar part of the surface energy decreases with increasing bias voltage, and the tendency is consistent with the change of the I_D/I_G ratios. It is believed that this trend is affected mainly by the reduction of the content in the films. Activation and the quantity of adherent platelets on the surface of the a-C:H films are influenced by the substrate bias. The higher the bias V_b, the larger is the activation of the adherent platelets. This trend is consistent with the surface energy of the films. The effects can be attributed to the preference of albumin adsorption due to the higher W_a value of albumin compared to that of fibrinogen and the changes of fibrinogen conformation caused by higher interfacial energy γ_{sp}. The blood compatibility of the a-C:H film deposited at –75 V is better than that exhibited by stainless steel and similar to that of LTI-carbon.

5.3 The influence of annealing temperature on film characterics

Hydrogenated amorphous carbon films were fabricated at room temperature using plasma immersion ion implantation-deposition (PIII-D). After PIII-D, annealing was carried out at 200–600°C for 30 min at reduced pressure (<1 × 10^{-3}Pa).

The position and width of the G-peak and I_D/I_G ratio as a function of the annealing temperature are shown in Fig. 12. The shift in the G-band indicates the increase in size and number of the sp^2 carbons, and the increase in the observed I_D/I_G intensity ratio suggests that there is an increase in the number of ordered aromatic rings within the samples. The emergence of the D-band as well as the increase of the I_D/I_G ratio show that the material has become nano-crystalline graphite [15]. The steep changes observed in the three curves at 300–400°C indicate that graphitization is promoted at higher annealing temperature arising from a diffusive mechanism. Similar results have been reported by Ogwu [16].

The dependence of *Eg*, resistivity and carrier concentration on annealing temperature is shown in Fig. 13. As the band gap does depend on the configuration of the sp^2 sites, the growth of the sp^2 cluster with increasing annealing temperature is the main reason for the observed

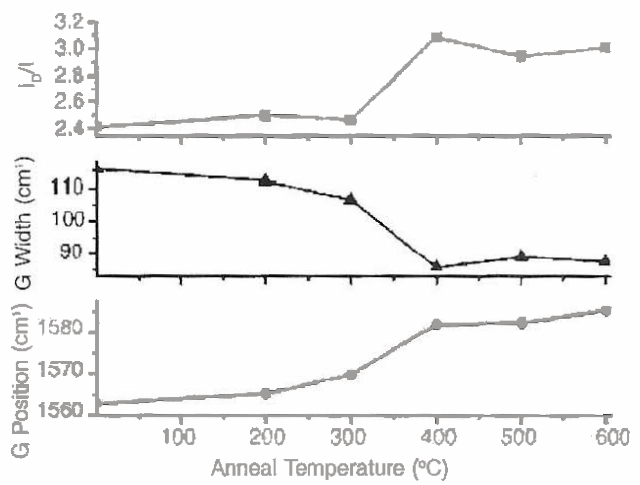

Fig. 12. Intensity ratios of the D-band to G-band, width and position of G-band with annealing temperature derived from Raman spectra.

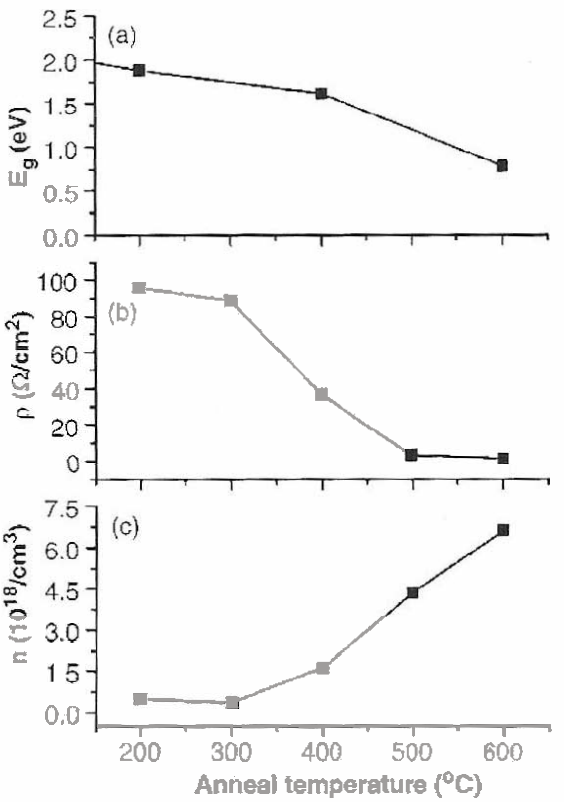

Fig. 13. Band gap, resistivity, Hall mobility and carrier concentration of a-C:H films as functions of annealing temperature.

band gap narrowing [17]. Both the resistivity and Hall mobility decrease with increasing annealing temperature and the trends are consistent with the Raman shift of the G-line. The steep changes approximately 400°C in the two curves also agree with the Raman results. Thus, it appears that the increase of the electrical conductivity in the annealed a-C:H film is related to an increase in the sp^3 bonding carbon and ordered sp^2 cluster caused by graphitization.

Fig. 14 exhibits the statistical results of the platelets adhered on the a-C:H films of different anneal temperature from PRP. In contrast with the results acquired from the as-deposited film, the number of adherent platelets on the annealed films decreases, fluctuates slightly from 200 to 500°C, and increases slightly at 600°C. The un-activated platelet percentages of the annealed films are close to that of as-deposited one when the annealing temperature is lower than 400°C, and the percentages decrease when the anneal temperature is higher than 500 8C. The curvechanges steeply at 400–500°C like the curves in Fig. 14. It thus appears that annealing at a relatively low temperature cannot cause retrogression of blood-compatibility of our a-C:H films, and the activation of platelets adhered on the a-C:H film surfaces is related to the change of the physical properties of the films.

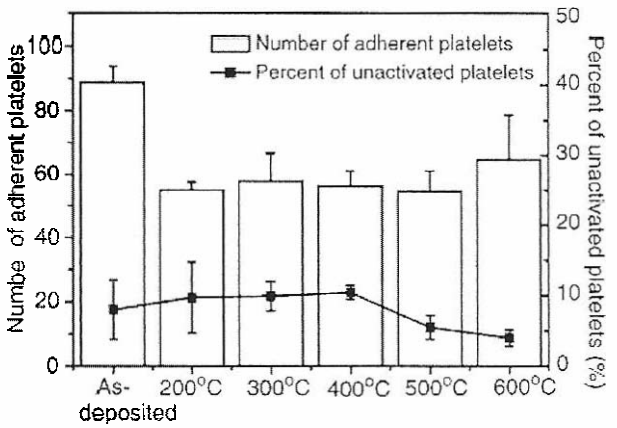

Fig. 14. Quantity of platelets adhered on the surface of the a-C:H films annealed at different temperature (15 min incubation in PRP).

When blood comes in contact with an artificial surface, the first event is protein adsorption. If the adsorbed protein such as fibrinogen is denatured, the coagulation factors or platelets will be activated causing a series of cascade reaction of blood coagulation and finally thrombosis. It has been shown that denaturing of fibrinogen and coagulation factor FV, FVIII, FIX depends on transfer of its charges to the material, and this process is related to the electronic structure and properties of the material [18,19]. Fibrinogen has an electronic structure similar to that of a semiconductor. When a material possesses a wider band gap than fibrinogen, there are less local states in the band gap, lower carrier concentration and n-type structure, and consequently, fibrinogen denaturation will be inhibited. Thus, it is reasonable that the as-deposited a-C:H film with a larger band gap and lower carrier concentration possesses lower surface activation of adherent platelets. It is probably the reason for the blood-compatibility retrogression at temperature higher than 400°C and the significant change in the electronic characteristics such as narrowing of the band gap (narrower than band gap of fibrinogen), order-of-magnitude increase of the carrier concentration and of p-type conductivity. Hence, the blood compatibility of a-C:H films is affected by the electronic structure and improving the electronic structure is important for the abatement of platelet activation.

6. *Blood platelet behaviors on elemental doped DLC*

6.1 Phosphorus doped DLC films (P-DLC)

Phosphorus is commonly found in inorganic phosphate rocks and in all living cells, it is one of the essential elements in biological system. In the study, DLC films were firstly fabricated using acetylene gas in PIII-D instrument. Subsequent P implantation was conducted in the same vacuum chamber using high-voltage glow discharge so as to prepare P-doped DLC.

Dotlike features are observed in the phosphorus doped DLC films as depicted in Fig. 15. These microstructures with an average diameter of 8–18 mm and height of 30–50 nm are evenly distributed near the film surface. The total solid-surface free energy and its components were determined using double-distilled water and diiodomethane. The surface free energy components of different materials and biological substances are summarized in Table 1. For the P-doped DLC film, the total surface free energy increases from 42.9 to 72.4 nJ/cm^2 and the polar component (γ_s^p) increases from 11.5 to 44.8 nJ/cm^2. Moreover, the contact angle of water

drastically diminishes to 16.98. These data indicate that the wettability is improved by phosphorus doping.

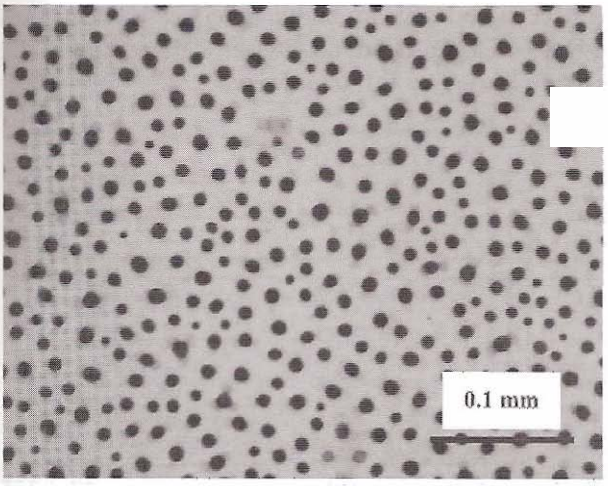

Fig. 15. Optical micrograph of the surface of P-doped DLC.

Table 1. Contact angle and surface energy components of different materials and biological substances.

Substrate	Contact angle		Surface energy (mJ/m^2)		
	Water	Diiodomethane	γ_s	γ_s^d	γ_s^p
LTIC	74.9	34.4	43.1	37.5	5.6
DLC	68.4	43.8	42.9	31.4	11.5
P doped DLC	16.9	37.0	72.4	27.6	44.8
Blood	-	-	47.5	11.2	36.3
Fibrinogen	-	-	65.0	24.7	40.3
Albumin	-	-	65.0	31.38	33.62

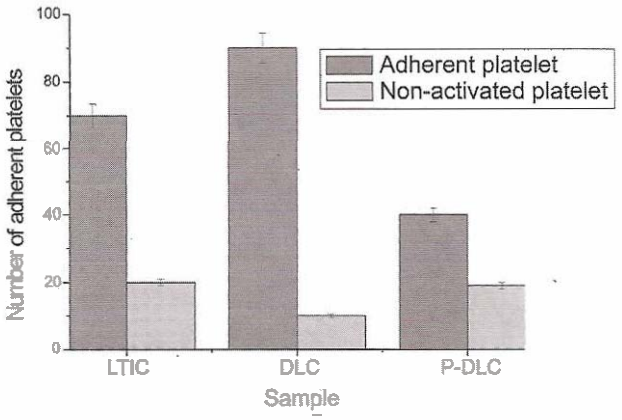

Fig. 16. Quantity of platelets adhered on the surface of LTIC, DLC and P-doped DLC.

Fig. 16 displays the statistical amount of adherent platelets on low-temperature isotropic pryolytic carbon (LTIC), undoped DLC, and P-doped DLC films after 20-min incubation. It has recorded that the number of adherent platelets on the P-doped DLC film is lower than that on LTIC which is a common biomedical material. The morphology of adhered platelets was assessed and the platelets shape changes on the different surfaces after 120 min incubation are compared. As shown in Fig. 17, the adherent platelets on the P-doped DLC (Fig. 17b) and LTIC (Fig. 17a) are isolated and relatively round.

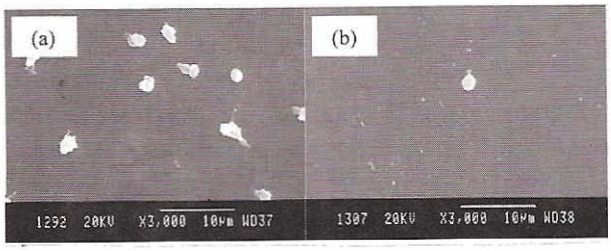

Fig. 17. (a) Morphology of adherent platelets on LTIC (120-min incubation in PRP) observed by SEM; (b) morphology of adherent platelets on P-doped DLC (120-min incubation in PRP) observed by SEM.

In the study, it has found that the interfacial tension is highest with albumin on the P-doped DLC film, but there are higher interfacial tensions between fibrinogen and LTIC or DLC. This suggest that albumin is preferentially adsorbed on P-doped DLC, whereas fibrinogen is preferentially adsorbed on LTIC and DLC. In particular, a high contribution of a polar interaction between undoped DLC and albumin and an equal level of dispersive and polar interaction between undoped DLC and fibrinogen further prove the preferential adsorption of fibrinogen on the undoped DLC surface. Albumin preferential adsorption is known to passivate the surface of an implant and the preferential adsorption of fibrinogen or globulin will lead to favor coagulation and platelet activation. Furthermore, the interfacial tensions of three kinds of plasma proteins on the P-doped DLC surface are significantly lower than those on the undoped DLC and LTIC surface. Moreover, a mechanically stable blood–biomaterial interface is considered another surface energetic criterion of biocompatibility of a foreign surface [20]. Because the cellular elements are compatible with blood and their interface with the medium is also mechanically stable, it is considered that a blood–biomaterial interfacial tension of about the same

magnitude as the cell–medium interfacial tension ($\gamma_{SL} \approx$ 1-3 dyn/cm) will provide a foreign surface with both long-term compatibility as well as mechanically stable interface with blood. It has shown that the interfacial tension between the P-doped DLC film and medium (water) is 2.7 dym/cm, which has the same magnitude as the cell–medium interfacial tension. Thus, the good hemocompatibility of the P-doped DLC coating is that it has significantly minimizes the interactions with plasma protein giving rise to slight changes in the conformation of adsorbed plasma proteins and preferentially adsorbed albumin.

6.2 Calcium doped DLC films (Ca-DLC)

Calcium (Ca) is the fifth most abundant element in the earth crust and it is one of the essential elements in living organisms particularly pertaining to cell physiology. Moreover, calcium is a crucial constituent in bones and teeth formation hence it is a interesting dopant in DLC for biomedical applications. In this study, three doped DLC films: Ca doped, Ca & P doped, and P doped DLC films were deposition.

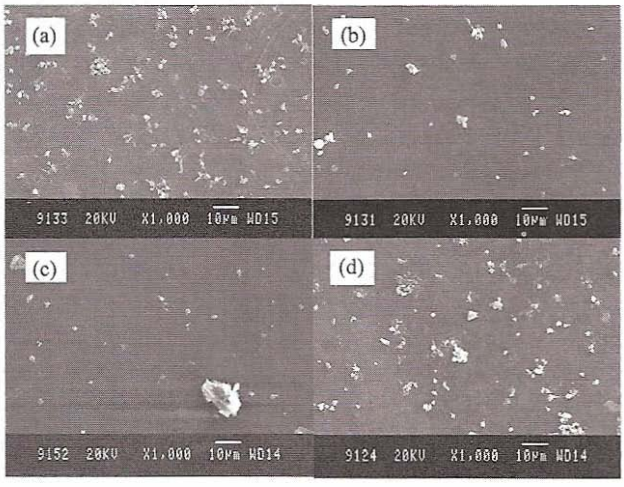

Fig. 18. SEM photos showing adhered platelets on (a) CaP-DLC, (b) P-DLC, (c) Ca-DLC, and (d) LTIC control.

The surface biocompatibility was assessed using in vitro platelet adhesion tests. Fig. 18 displays the morphology and the quantity of the adhered platelets on the samples. The statistical results are presented in Fig. 19. Both the P-DLC and Ca-DLC films show smaller numbers of adhered and unactivated platelets than LTIC. Our results show that either Ca or P doping alone can enhance the hemocompatibility but not when acting together. Figs. 20–22 display the XPS depth profiles acquired from the Ca, P, and Ca-P doped DLC films, respectively. The Ca-DLC profile shows a sharp film interface at about 25 nm but the interfaces in the P and Ca-P doped samples are not as well defined due to the interface mixing by PIII treatment.

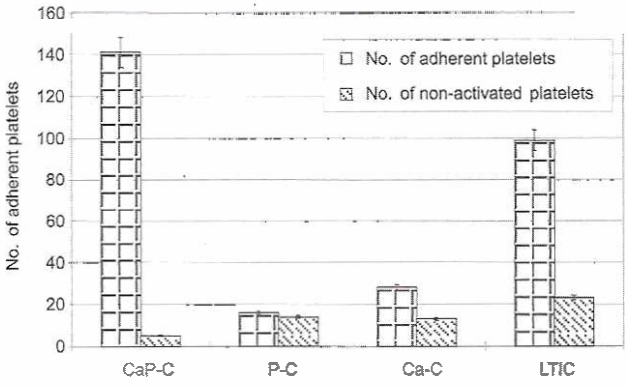

Fig. 19. Quantity of platelets adhered on CaP-C, P-C, Ca-C and LTIC.

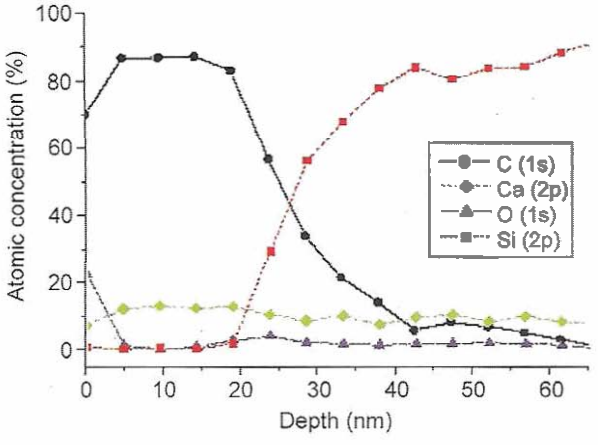

Fig. 20. Elemental depth profiles acquired from the Ca-DLC film.

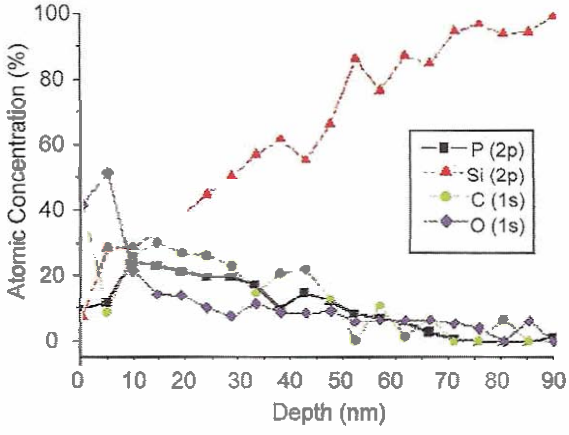

Fig. 21. Elemental depth profiles acquired from the P-DLC film.

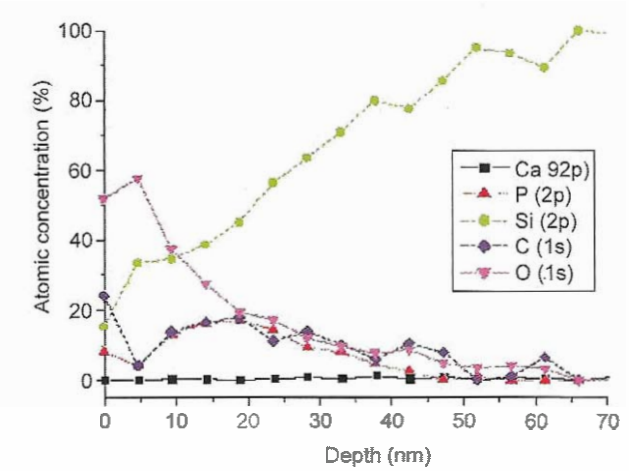

Fig. 22. Elemental depth profiles obtained from the CaP-DLC film.

The interfacial energies (γ_{sp}) between plasma proteins and samples are shown in Table 2. Ca-DLC (0.11) and P-DLC (0.08) have lower value of $\gamma_{sp}^{p}/\gamma_{sp}^{d}$ for albumin (γ_{sp}^{p} and γ_{sp}^{d} represent the polar and dispersive components of the interfacial energy between proteins and materials) than CaP-DLC and LTIC, suggesting stronger adhesion of albumin. The $\gamma_{sp}^{p}/\gamma_{sp}^{d}$ ratio for fibrinogen is also small, but the total interfacial energy, γ_{sp}, is less than that of albumin, which means that less conformational changes occur. The results suggest that these surface energies are the primary factors for the good compatibility observed on Ca-DLC and P-DLC in the platelet adhesion test. Table 3 shows the results of the contact angles and calculated interfacial energies (γ_{sw}) between water and the films. Ca-DLC and P-DLC have the lowest value of interfacial energy (γ_{sw} =6.2 and 5.1, respectively) with water (medium), indicating that both films have closer interracial tension (1–3 nJ/cm^2) with the cell medium than CaP-DLC and LTIC. Hence, the platelet results are consistent with the calculated surface energy.

Table 3. Contact angle (θ_w) and interfacial energy (γ_{sw}) between different materials (samples) and water.

Materials	θ_w (°)	γ_{sw} (nJ/cm^2)
Ca-DLC	87.2	6.2
CaP-DLC	51	57.6
P-DLC	49	5.1
LTIC	74.9	24.2

7. Conclusion

Much progress has been made in the improvement of blood compatibility of biomaterials using plasma immersion ion implantation and deposition. In the study, the influence of flow rate, bias voltage and annealing temperature on the characteristics of DLC and the further improvement of blood compatibility of doped DLC have been investigated.

Reference

[1] R. Hauert, *Diamond Relat. Mater.* **12 (3–7)** (2003) 583–589.

[2] A. Grill, *Diamond Relat. Mater.* **12** (2) (2003) 166– 170.

[3] F.Z. Cui, D.J. Li, *Surf. Coat. Technol.* **131** (2000) 481– 487.

[4] M. Allen, B. Myer, N. Rushton, *J. Biomed. Mater. Res.* **58** (2001) 319.

[5] D.P. Dowling, P.V. Kola, K. Donnelly, T.C. Kelly, K. Brumitt, L. Lloyd, *Diamond Relat. Mater.* **6** (1997) 390.

[6] N.J. Ianno, R.O. Dillon, A. Ahmad, A. Ali, *Thin Solid Films* **270** (1995) 275.

[7] J. McLaughlin, B. Meenan, P. Maguire, N. Jamieson, *Diamond Relat. Mater.* **5** (1996) 486.

[8] J. Robertson, E. P. O'Reilly, *Phys. Rev.* **B 35** (1987) 2946.

[9] G. P. Lopinski, *Phys. Rev. Lett.* **80** (1998) 4241.

[10] J. Schwan, S. Ulrich, V. Batori, *et al. J. Appl. Phys.* **80** (1994) 440.

[11] D. Beeman, *et al. Phys. Rev.* **B 30** (1984) 870.

[12] L. Valentini, J. M. Kenny, P. Tosi, *et al. Diamond Relat. Mater* **10** (2001) 1042.

[13] K. H. Lai, C. Y. Chan, M. K. Fung, *et al. Diamond Relat. Mater.* **10** (2001) 1862.

Table2. Interfacial energies between materials and plasma proteins.

Biological substance	P-C (a)		P-C (b)		P-C (c)		P-C (d)	
	γ_{sp}	$\gamma_{sp}^{p}/\gamma_{sp}^{d}$	γ_{sp}	$\gamma_{sp}^{p}/\gamma_{sp}^{d}$	γ_{sp}	$\gamma_{sp}^{p}/\gamma_{sp}^{d}$	γ_{sp}	$\gamma_{sp}^{p}/\gamma_{sp}^{d}$
Fibrinogen	9.6	0.18	6.7	0.04	12.6	0.24	3.9	1.44
Albumin	15	0.26	11	0.11	19	0.30	4.5	0.26

[14] F. Pinzari, P. Ascarelli, E. Cappelli, G. Mattei, R. Giorgi. *Diamond Relat. Mater.* **10** (2000) 781.

[15] Z. Tang, Z.J. Zhang, K. Narumi, Y. Xu, H. Naramoto and S. Nagai, *J. Appl. Phys.* **89** (2001) 1956.

[16] A.A. Ogwu, R.W. Lamberton, S. Morley, P. Maguire and J. Mclaughlin, *Physica* **B 269** (1999) 335.

[17] J. Robertson, *Mater. Sci. Eng. Rep.* **37** (2002) 129.

[18] L. Feng and D.J. Andrade, *J. Colloid Interface Sci.* **166** (1994) 419.

[19] N. Huang, P. Yang, X. Cheng, Y. Leng, X. Zheng, G. Cai, *et al., Biomaterials* **19** (1998) 771.

[20] E. Ruckensten, S.V. Gourisankar, *J. Colloid Interface Sci.* **101** (2) (1984) 436– 451.